

This article was downloaded by:

On: 25 January 2011

Access details: *Access Details: Free Access*

Publisher *Taylor & Francis*

Informa Ltd Registered in England and Wales Registered Number: 1072954 Registered office: Mortimer House, 37-41 Mortimer Street, London W1T 3JH, UK



Separation Science and Technology

Publication details, including instructions for authors and subscription information:

<http://www.informaworld.com/smpp/title~content=t713708471>

SRS Low-Curie Process Modeling and Experiments

L. T. Smith^a; R. K. Toghiani^b; A. Antonyraj^c; V. Phillips^a; J. S. Lindner^a

^a Institute for Clean Energy Technologies, Mississippi State University, MS, USA ^b Dave C. Swalm School of Chemical Engineering, Mississippi State, MS, USA ^c Agricultural and Biological Engineering, Mississippi State, MS, USA

To cite this Article Smith, L. T. , Toghiani, R. K. , Antonyraj, A. , Phillips, V. and Lindner, J. S.(2006) 'SRS Low-Curie Process Modeling and Experiments', Separation Science and Technology, 41: 11, 2341 — 2360

To link to this Article: DOI: 10.1080/01496390600745446

URL: <http://dx.doi.org/10.1080/01496390600745446>

PLEASE SCROLL DOWN FOR ARTICLE

Full terms and conditions of use: <http://www.informaworld.com/terms-and-conditions-of-access.pdf>

This article may be used for research, teaching and private study purposes. Any substantial or systematic reproduction, re-distribution, re-selling, loan or sub-licensing, systematic supply or distribution in any form to anyone is expressly forbidden.

The publisher does not give any warranty express or implied or make any representation that the contents will be complete or accurate or up to date. The accuracy of any instructions, formulae and drug doses should be independently verified with primary sources. The publisher shall not be liable for any loss, actions, claims, proceedings, demand or costs or damages whatsoever or howsoever caused arising directly or indirectly in connection with or arising out of the use of this material.



SRS Low-Curie Process Modeling and Experiments

L. T. Smith

Institute for Clean Energy Technologies, Mississippi
State University, MS, USA

R. K. Toghiani

Dave C. Swalm School of Chemical Engineering,
Mississippi State, MS, USA

A. Antonyraj

Agricultural and Biological Engineering,
Mississippi State, MS, USA

V. Phillips and J. S. Lindner

Institute for Clean Energy Technologies, Mississippi
State University, MS, USA

Abstract: Engineers at SRS are evaluating the Low-Curie Salt Process which is aimed at initially withdrawing the interstitial liquor followed by dissolution of the salt cake. Partitioning of the cesium is predominantly within the interstitial liquor; consequently a separation based on activity can be effected. Laboratory experiments using simulants from SRS tanks have been performed along with thermodynamic simulations. Results indicate that insoluble layers such as Al(OH)_3 and/or cancrinite may form and hinder the dissolution processes. The effectiveness of the Low-Curie Salt Process may be reduced based on layer formation and the distribution of the interstitial liquor within the waste.

Keywords: Cesium, DASR (Drain, Add, Sit, Remove), thermodynamic modeling, nuclear waste processing, salt cake, dissolution

Received 27 October 2005, Accepted 17 March 2006

Address correspondence to L. T. Smith, Institute for Clean Energy Technologies, Mississippi State University, P.O. Box 9550, Mississippi State, MS 39762, USA.
E-mail: lsmith@icet.msstate.edu

INTRODUCTION

Currently, over 35 million gallons of legacy nuclear waste are stored in 49 underground storage tanks at the Savannah River Site. In 2002, SRS developed an Environmental Management Program Performance Management Plan (PMP) for High Level Waste (HLW) (1). This program included a tailored-treatment concept to partition the HLW into four fractions, thereby reducing processing time and associated costs. The four fractions include:

- Sludge (which includes the largest concentrations of long-lived radionuclides),
- Low Curie Salt,
- Low Curie Salt with higher actinide concentrations and,
- High Curie Salt with higher actinide concentrations.

The Low Curie Salt (LSC) fraction is separated from the remaining fractions by removing the interstitial liquid from selected tanks in the H tank farm. The majority of the cesium is found in this interstitial liquid, thereby effecting a separation, with very little cesium remaining in the salt cake. Solubility estimates for cesium predict the activity of a saturated cesium solution to be 10,738 Ci/gallon (0.243 M Cs). The measured activity level for SRS interstitial liquids is between 0.2 and 0.9 percent of the solubility at saturation (2). This indicates that removal of the interstitial liquid will, in fact, partition the cesium into a fraction of smaller volume, compared to the entire tank contents. The remaining salt cake is then dissolved using dilution water or using an available stream from other operations (3). The dissolved salt cake solution is then sent to Tank 50 for interim storage. There, the composition is compared to the Saltstone Waste Acceptance Criteria (WAC), with the planned disposal of the waste as grout. The Low Curie Process was approved and operations began in 2003.

EXPERIMENTAL

The experimental setup was designed to imitate as closely as possible the Low Curie Salt process. The 3-in ID column was seven inches tall, and constructed of clear acrylic. A calibration scale (machine etched) for height was available on the exterior of the vessel and was used to monitor the level of the salt cake/interstitial brine in the column (4). A tube placed between the center and far wall of the column was used to mimic a salt well. This tube (Fig. 1) was fashioned from a polypropylene round bottom culture test tube (13 × 100 mm), and had approximately 32 spaced holes drilled through the tube wall near the lower portion of the tube but none in the curved bottom. These holes allowed interstitial liquid to drain from the



Figure 1. Schematic of polypropylene tube used as salt well in DASR experiments. (Holes and tube are not drawn to scale).

salt cake into the well where it could be removed by pumping. A Cole-Palmer Masterflex model 77390-000 peristaltic pump was used to pump the retrieved liquid into a collection vial. All DASR experiments were performed in an ETS controlled environment chamber (model 532) at temperatures of 25°C or of 30°C. The experimental temperature was selected based on the actual waste temperature for a given tank.

Salt Cake Simulant Preparation

Simulants representative of the salt waste compositions for SRS Tanks 41H (5), 38H (6), and 37H (7) were developed in collaboration with SRS engineers. The simulant recipes are given in Table 1. Each recipe was sufficient to prepare simulant for at least two DASR experiments. Preparation of a simulant for laboratory use requires the sequential dissolution of all constituents at temperatures greater than 50°C followed by evaporation and cooling. The dissolution was performed in a 3L stainless steel beaker using a heating plate equipped with a magnetic stirrer and excess water to promote complete dissolution of the constituents. Stirring was continuous during chemical additions. The temperature of the solution containing all of the required constituents was then increased to 110°C. Water was evaporated from the solution, until a pre-specified volume was attained. This resulted in a brine that, upon cooling, would yield a salt waste with a known water loading.

Table 1. SRS 41H, 38H, and 37H simulant recipes (All quantities in grams)

Constituent	Tank 41H	Tank 38H	Tank 37H
NaNO ₃	58.6	56.5	27.00
Na ₂ CO ₃	8.95	5.84	29.0
NaAlO ₂ · 2.5H ₂ O	8.33	0.51	3.23
NaOH	3.60	4.62	1.75
NaNO ₂	1.75	2.70	1.49
Na ₃ PO ₄ · 12H ₂ O · 0.25 NaOH	1.54	0.074	1.29
Na ₂ SO ₄	1.29	2.35	0.56
Na ₂ SiO ₃	0.00	0.10	3.74
Na ₂ C ₂ O ₄	0.19	0.69	0.00
NaCl	0.04	0.014	0.00
NaF	0.00	0.077	0.00
H ₂ O	15.7	26.5	35.7
Total grams	100.0	100.005	103.7

The brine solution was then cooled, resulting in the precipitation of salts, yielding a salt waste in slurry form.

The prepared salt waste simulant was maintained at either 25°C (or 30°C) and allowed to age for a period of not less than 4 days. Previous work in this laboratory has demonstrated that crystal ripening can affect the resulting particle size distributions of sodium phosphate crystals. During this ripening period, the salt waste will settle, leaving a layer of free brine above the porous salt waste matrix. Prior to addition of the salt waste to the small column, the entire batch of simulant was stirred to ensure that the material poured into the small column was uniform in composition. Our laboratories are equipped with a thermal gravimetric analyzer (TGA). This unit allows the evaluation of the percent water by weight in a given sample, by determining the mass of water evolved from a sample during a programmed increase in temperature. This experimental measurement was essential input to the dissolution modeling, used to set the water content of the input stream.

Salt Cake Drain, Add, Sit, and Remove Module (DASR) Experiments

The DASR experimental procedure was developed to mimic the SRS process as closely as possible. In these experiments, the acrylic column, having a millimeter calibration scale, are equipped with a fitted Teflon stopper affixed to the lower portion of the column to prevent flow. The column was then placed in the environmental chamber which was preset to

a constant temperature. The salt cake was poured into the column and allowed to settle under the influence of gravity. The free supernatant (the liquid sitting atop the settled salt cake) was removed using the peristaltic pump. A well was created in the salt cake by insertion of a fraction collector tube (Fig. 1) to the bottom of the salt bed.

The interstitial liquid that drained into the well was removed using the peristaltic pump. Generally, brine was collected every 6 hours over a period of two to three days to allow sufficient time after each collection for the interstitial liquid to drain into the well and to retrieve as much of the interstitial liquid possible based on the location of the drilled holes within the tube. The bottom section of the tube was curved; consequently, the bottommost portion of the salt cake with trapped interstitial liquid was not able to drain. As time progressed, smaller and smaller volumes of interstitial liquid drained into the well and were removed. When the volume of interstitial liquid draining into the well was reduced sufficiently, indicating that the greater portion of drainable interstitial liquid had been removed from the salt cake, the drainage of interstitial liquid was halted.

At this point, the dissolution portion (add and sit) of the experiment was initiated. A piece of Whatman (#542) 110 mm diameter, hardened ashless filter paper was sized to completely cover the cross sectional area of the column. It was placed atop the surface of the salt cake. A known mass of diluent was then added, by slowing dripping the diluent onto the filter paper again using the peristaltic pump. Previous experiments had shown that the filter paper tended to disperse the diluent across the entire cross sectional area of the column, thereby reducing the possibility of channeling. Channeling is a potential problem if the diluent is strictly added at one location on the surface. The diluent was added at a 1 mL/minute flow rate for ten minutes and allowed to interact with the simulant over a 24-hour period. After the 24-hour interval, the dissolved salt solution was removed from the well using the peristaltic pump and collected in a weighed, labeled vial. The height of salt cake in the column was measured and recorded. This procedure (diluent addition, removal of dissolved salt solution) was then repeated until the height of salt cake in the column had dropped below a measurable value. A portion of each sample collected was prepared for chemical analysis by dilution. Sequential fractions were also combined to obtain information on feed stability and the possibility of reprecipitation of solids when the liquid fractions were recombined. Analytical methods used for the analysis are listed in Table 2.

Thermodynamic Calculations

The Environmental Simulation Program (ESP, OLI Systems Inc.) was used to predict the solid-liquid equilibria of the constituents within the salt cake. Simulation of a given process began with the development of a chemistry

Table 2. Supporting instrumentation for the DASR experiments

Method	Analysis
Ion chromatography (IC)	NO_2^{-1} , NO_3^{-1} , SO_4^{-2} , PO_4^{-3} , Cl^{-1} , F^{-1} , $\text{C}_2\text{O}_4^{-2}$
Inductively coupled plasma spectrometry (ICP)	Al^{+3} , Si
Total inorganic and organic carbon (TIC/TOC)	CO_3^{-2}
Polarized light microscopy (PLM)	Solids identification and size
Thermal gravimetric analysis (TGA)	Supernatant and salt cake water loading

model that contained all of the molecules and ions of interest. For this task a number of databases relating to specific chemistry can be called. Previous work in these laboratories has focused on the determination of solubilities for a number of systems pertinent to salt cake waste. These data, typically obtained in water, 1 m, and 3 m caustic at 25 and 50°C, were determined at various loadings and then analyzed in the Bromley formalism for development of a specific ESP private databank (8). The double salt databank (DBSLTDB) contains information on the compounds listed in Table 3. This database was used in this work and version 6.5 of the software was employed. The Silicat database, available from OLI Systems Inc, and the Zeolite database (obtained from SRS personnel) were also used for modeling when both silicon and aluminum were present.

The flow sheet included the preparation of the simulant according to the laboratory procedure and the dissolution of the salt cake based upon the DASR experimental configuration. Approximately 1L of the salt matrix was prepared and TGA experiments conducted on the slurry to determine the percent water by weight. The fraction of free water was then adjusted in the ESP flow sheet through either the temperature at which evaporation occurred or by using a single component split block. The water content within ESP was tuned to the experimental results.

Table 3. Compounds utilized for solubility studies and database development

NaNO_3	NaF
NaNO_2	Na_3FSO_4
$\text{Na}_2\text{SO}_4 \cdot x\text{H}_2\text{O}$	$\text{Na}_3\text{PO}_4 \cdot 12\text{H}_2\text{O} \cdot 0.25\text{NaOH}$
$\text{Na}_2\text{CO}_3 \cdot x\text{H}_2\text{O}$	$\text{Na}_7(\text{PO}_4)_2 \cdot 19\text{H}_2\text{O}$
$\text{Na}_6\text{CO}_3(\text{SO}_4)_2$	$\text{Na}_3\text{NO}_3(\text{SO}_4) \cdot \text{H}_2\text{O}$

RESULTS AND DISCUSSION

Salt Cake Composition and ESP Calculations

Specific properties for the base compositions of Tank 41H, 38H, and 37H salt cake simulants calculated using ESP are compiled in Table 4. The calculations include the percent of water by weight and do not include the addition of any diluent. The overall (bulk) solids density was calculated based on the mass of each solid predicted and the pure component density. Densities for a number of solids are not included within the ESP package. Tank 41 results have been reported previously (9) and are used here for comparison.

ESP modeling of the experimental procedure followed a standard flowsheet as given in Fig. 2. The model simulant was prepared, separated based upon the experimental mass transferred to the column and the free and the bulk of the interstitial fluid masses were removed before diluent addition. The column height was measured (for volume) using digital images of the scale on the acrylic column. This portion of the experiment is identified as Waste prep in the flowsheet. The addition of the diluent (water) was followed by a separation in order to remove the dissolved salt

Table 4. ESP model predictions for the SRS Tank 41H, 38H, and 37H simulants without diluent addition

Tank basis	41H	38H	37H
Supernatant properties			
Density (g/mL)	1.48E + 00	1.43E + 00	1.36E + 00
pH	1.51E + 01	1.52E + 01	1.48E + 01
Ionic strength	1.71E + 01	1.35E + 01	1.07E + 01
Abs viscosity (cP)	1.41E + 01	6.50E + 00	5.30E + 00
Solid (%)			
Al(OH) ₃	1.04E + 01		
Na ₂ C ₂ O ₄	3.00E - 01	1.36E + 01	
Na ₂ CO ₃ · 1H ₂ O	8.10E + 00	5.76E + 00	6.68E + 01
Na ₂ SO ₄	1.89E + 00		
NaNO ₃	7.85E + 01	7.55E + 01	2.24E + 01
Na ₃ PO ₄ · 12H ₂ O · 0.25NaOH	8.10E - 01		2.10E + 00
Na ₆ (SO ₄) ₂ CO ₃		5.00E + 00	
Na ₂ F(PO ₄) ₂ · 19H ₂ O		6.60E-02	
Na ₃ FSO ₄		2.00E-01	
Cancrinite			8.70E + 00
Solids density (g/mL)	2.24E + 00	2.28E + 00	2.25E + 00
Salt cake properties			
Density (g/mL)	1.82E + 00	1.75E + 00	1.69E + 00
Weight % solids	5.20E + 01	4.91E + 01	4.03E + 01
Weight % water	2.42E + 01	2.75E + 01	3.94E + 01

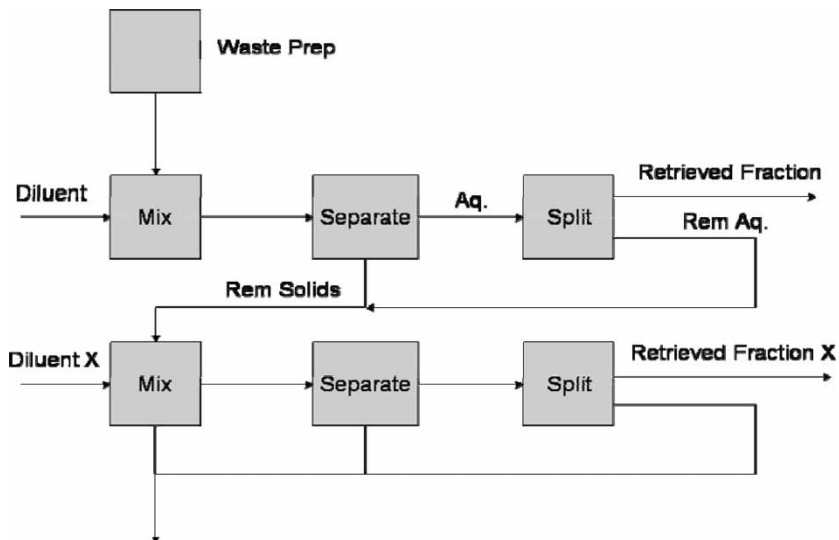


Figure 2. ESP standard flowsheet diagram for the DASR experiment.

fraction in a split block. The solids and remaining aqueous portion are mixed back together for the next diluent addition and the process repeated until the experiment is completed.

SRS Tank 38H Simulant Experiment Physical Results

The simulant for 38H was prepared following the procedures described above and left to age approximately 4 days. The simulant was re-slurried and a sample removed for analysis in order to obtain the percent water by weight. The water loading determined by TGA measurements averaged a value of 27.8%. About 75% of the total solids mass predicted by the model (tuned to the percent water obtained experimentally) was calculated to be present as sodium nitrate. Additional solids of some importance included sodium carbonate monohydrate, sodium oxalate and the sodium-sulfate-carbonate, natrophosphate and sodium fluorosulfate double salts, Table 4. The simulant is similar in composition to 41H, having sodium nitrate as the predominate solid, but contains a larger weight percent (13.6%) of sodium oxalate and double salts not predicted for the 41H simulant.

Two identical DASR experiments were performed and compared due to unusual behavior of the experimental sodium nitrite profiles. Masses and volumes associated with the experiments are collected in Table 5. The two entries concern the initial separation of the free supernatant and the interstitial liquor from the simulant charge and the mass balance for the entire

Table 5. Pertinent results from the DASR experiments on the SRS Tank 38H salt cake simulant. Results from the DASR experiment for 41H simulant are included for comparison

Diluent	Water		
	DASR 38H 1	DASR 38H 2	DASR 41H
Interstitial liquid recovery			
Initial mass of simulant (g)	526.18	483.77	654.50
Initial volume of simulant (cc)	297.4	219.89	339.12
Free supernatant mass (g)	118.37	115.103	58.47
Free supernatant volume (cc)	83.36	81.06	39.51
Mass interstitial liquid collected (g)	57.98	32.03	106.25
Volume interstitial liquid collected (cc)	40.83	21.5	71.79
Inaccessible salt cake volume (cc) ^a	36.46	36.46	36.46
Interstitial liquid expected ^b (cc)	54.32	44.43	98.82
% Interstitial liquid collected	73.6	52.93	72.64
Total experiment duration (days)	16	15.3	9
Mass balance			
Mass of SC before dilution (g)	349.83	336.64	489.78
Mass diluent added (g)	176.15	170.12	351.20
Total mass in (g)	525.99	506.76	840.98
Mass of liquid collected (g)	405.54	348.02	750.27
Mass of SC remaining at end (g)	90.90	111.34	78.00
Total mass out (g)	496.44	459.36	828.27
Recovery (%)	94.38	90.65	71.70

^aThis is the volume associated with the height of the lowest drain holes in the well, below which involves indirect mixing and no draining is possible.

^bAssuming a salt matrix porosity of 32%.

experiment. In determining the percentage of the interstitial fluid recovered it was assumed that the simulant salt matrix had a porosity of 32%. Previous experiments to determine porosity of differing simulant compositions containing large weight percent sodium nitrate were performed and the results obtained gave an average value of 32% (9). A decrease in this value would lead to a lower mass or volume of interstitial liquid expected, which, in turn, would lead to a larger interstitial liquid percent recovery. In any case, the value of 73% interstitial recovery for experiment one is close to that targeted (75%) by SRS personnel (1) in performing DASR on waste in the actual tank. A lower interstitial recovery (52.9%) was obtained for experiment two.

Total experimental times are also shown for the runs. These have little practical meaning as different withdrawal rates and sit or dissolution times were employed. These durations illustrate that extensive times were allowed to achieve dissolution and that associated solids dissolution kinetics can be neglected.

Reported mass recoveries should be considered estimates. Typically there remains some salt bed toward the end of the experiment in pockets over the bottom plug in the column. These are retrievable by changing the location of the pores within the well, however, that was not performed in these experiments.

Since cesium and nitrite are found to be predominately in the aqueous phase, tracking the nitrite ion concentration during the dissolution process can be an indicator of how the cesium concentration will vary in the actual tank waste processes. Figures 3–5 compare the experimental and model nitrite ion concentrations in ppm-weight (ppmw) against the percent dissolution by weight. The similar 38H experimental results show anomalous behavior in the 17–30% dilution by weight region where the anion concentrations increase unexpectedly. The experimental data follow a decay, much like the predictions of the perfect mixing ESP (standard flowsheet) model. The experimental concentration is then seen to increase in the 17–25% dilution by weight range followed by a second decay. Results for the second DASR experiment confirmed the anomalous results for nitrite. Again a strong decrease in concentration is followed by an increase and then dilution decay. The nitrite anion is only predicted to be present in the

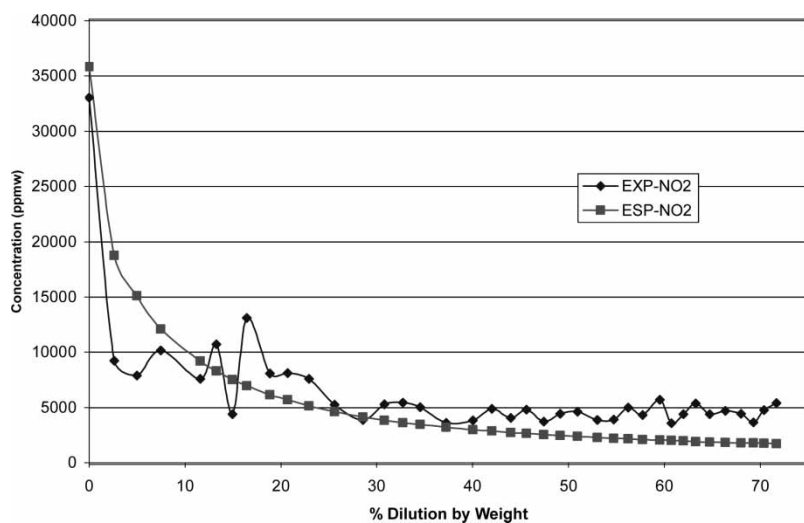


Figure 3. Comparison of experimental and predicted NO_2^- ion concentrations (ppmw) for Tank 41H experiment-standard flowsheet.

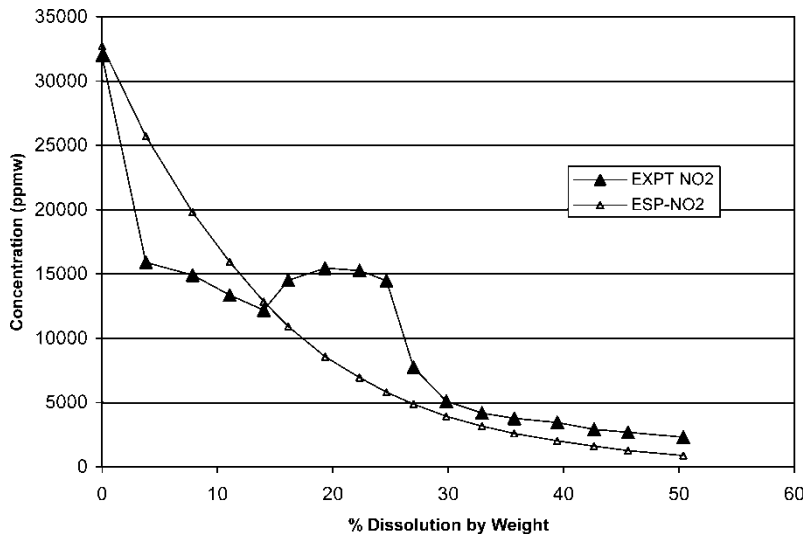


Figure 4. Comparison of experimental and predicted NO_2 ion concentrations (ppmw) for Tank 38H (DASR 1) experiment-standard flowsheet.

aqueous phase. The increase in any concentration as a function of dilution would imply the dissolution of solids.

A possible reason for the increase in the nitrite concentration is from the partial mixing of the salt cake interstitial liquor with the dissolved salt

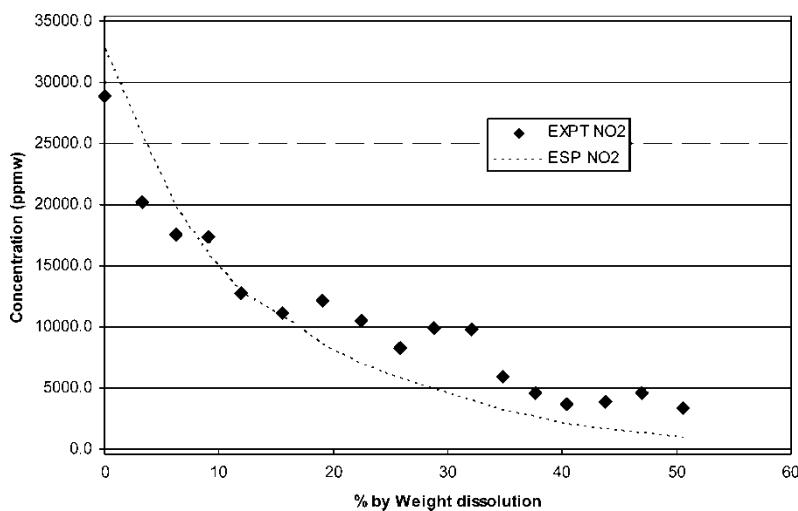


Figure 5. Comparison of experimental and predicted NO_2 ion concentrations (ppmw) for Tank 38H (DASR 2) experiment-standard flowsheet.

solution. Such a situation will be encountered when pockets of interstitial liquor are located in hard to retrieve areas of the column or of a waste tank. The second ESP (modified flowsheet) simulation was performed by controlling the mixing of the interstitial liquor with the dissolved salt solution. The modified flowsheet is shown in Fig. 6. The original solids were separated into layers and the brine fractions were set to generate the nitrite concentrations of the effluent collected. The number of layers generated for the solids were dependent upon the nitrate fraction concentrations.

The nitrite ion results obtained using the modified flowsheet are illustrated in Fig. 7 and indicate that the profile response can be attained through removal of the complete mixing assumption. Clearly, there may be no "a priori" reason to consider such an approach except in those practical situations where extensive draining of the interstitial liquor from a waste tank has occurred. In that case additional information regarding the hydrology of the waste would be useful; however, it is still possible to perform simulations at different extents of mixing and thereby develop ranges of potential concentrations in the dissolved salt solutions to be retrieved. The modified flowsheet provides agreement with the experimental results.

The nitrate and carbonate concentrations for both experiments show good agreement with each model used and a representative plot for one experiment is shown in Fig. 8. Both experiments have similar dilution fractions and concentration profiles. The salt cake consists of roughly 70% solid sodium nitrate; consequently the experimental profiles indicate an increase of nitrate anion as the solid is dissolved. The entire concentration profile was not observed as the dilutions were not extended to sufficiently high percentages by weight;

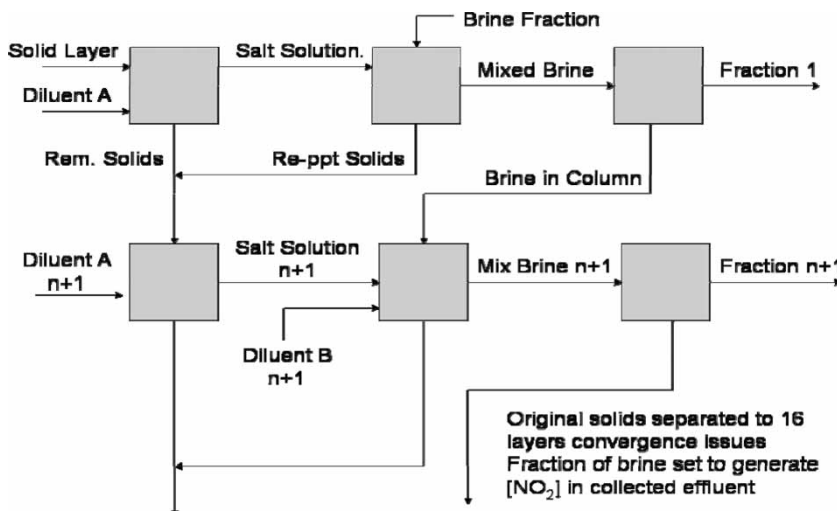


Figure 6. ESP modified flowsheet diagram for the DASR experiments.

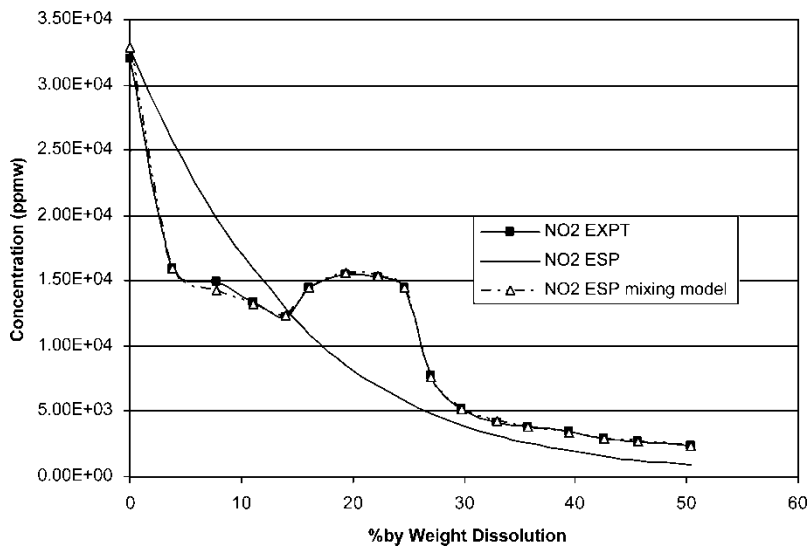


Figure 7. Comparison of experimental and predicted NO_2 ion concentrations (ppmw) for Tank 38H (DASR 1) experiment-standard and modified flowsheet.

however, both experimental profiles have achieved maximum concentrations and are tending toward the decay region. Similar comments apply to the carbonate anion profile. Radical changes in concentration as a function of dilution were not observed. Model predictions using the standard flowsheet and the modified flowsheet are essentially the same.

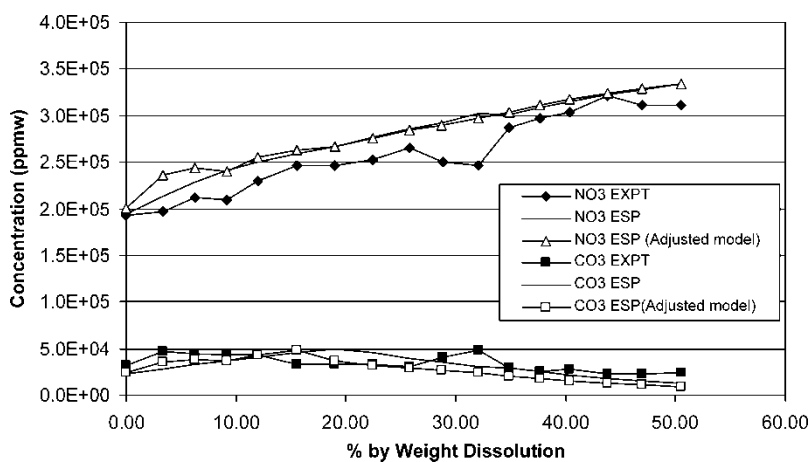


Figure 8. Comparison of experimental and predicted CO_3 and NO_3 ion concentrations (ppmw) for Tank 38H (DASR 2) experiment-standard and modified flowsheet.

SRS Tank 37H Simulant Experiment Physical Results

For the average SRS simulant composition, the prevalent solid is sodium nitrate with other sodium salts in smaller amounts. In both 41H and 38H simulants, the sodium nitrate solids constitute an average of approximately 77% of the total solids by weight. However, the 37H simulant consisted primarily of sodium carbonate monohydrate (66%) with sodium nitrate as a much lower constituent (22%). In addition, past results from SRS (10, 11) have identified the presence of sodium aluminum silicates, such as zeolite ($\text{Na}_6\text{Al}_{12}\text{Si}_{12}\text{O}_{48} \cdot x\text{H}_2\text{O}$ and/or $x(\text{NO}_3, \text{CO}_3)$), sodalite ($\text{Na}_8\text{Al}_6\text{Si}_6\text{O}_{24}(\text{NO}_2)_2$), or cancrinite ($\text{Na}_8\text{Al}_6\text{Si}_6\text{O}_{24}(\text{NO}_3)_2 \cdot 4\text{H}_2\text{O}$), when equal molar amounts of aluminum and silicon are constituents within high nitrate/nitrite solutions in the tank waste. This simulant composition includes all of these conditions. During the 37H simulant preparation, cancrinite solids that were predicted by the model were found experimentally. The simulant was re-slurried and a sample removed for analysis in order to obtain the percent water by weight. The water loading measurement

Table 6. Results from the DASR experiment on the SRS Tank 37H salt cake simulant

Diluent	Water (37H)
Interstitial liquid recovery	
Initial mass of simulant (g)	509.85
Initial volume of simulant (cc)	320.33
Free supernatant mass (g)	117.88
Free supernatant volume (cc)	83.6
Mass interstitial liquid collected (g)	36.86
Volume interstitial liquid collected (cc)	26.14
Inaccessible salt cake volume (cc) ^a	36.46
Interstitial liquid expected ^b (cc)	75.72
% Interstitial liquid collected	40.81
Total experiment duration (days)	50
Mass balance	
Mass of SC before dilution (g)	355.115
Mass diluent added (g)	391.00
Total mass in (g)	746.11
Mass of liquid collected (g)	610.60
Mass of SC remaining at end (g)	94.60
Total mass out (g)	705.20
Recovery (%)	94.52

^aThis is the volume associated with the height of the lowest drain holes in the well, below which involves indirect mixing and no draining is possible.

^bAssuming a salt matrix porosity of 32%.

provided an average value of 38%. Masses and volumes associated with the experiment are collected in Table 6.

The simulant was thoroughly slurried before placing in the column but a small layer formed on top of the solids. The cancrinite solids were observed to be very small particles and during the settling portion of the experiment formed a distinct layer across the entire salt cake as shown in Fig. 9. Interstitial recovery volume was low (40.8%) and the experimental duration compared to the 38H simulant experiments increased by a factor of 3. These values reflect a decreased permeability of the salt matrix and the potential for minimal diluent contact with the entire salt cake. A comparison plot of column height and time for the two simulants is shown in Fig. 10.

The nitrite ion concentration experimental profile, Fig. 11, did not demonstrate an increase as seen in the 38H experiment but the nitrate and carbonate ion experimental concentrations deviated considerably from the standard flowsheet model as shown in Figs. 12 and 13. In order to investigate these discrepancies between the model predictions and experimental results several approaches were attempted. First, all experimental results were verified by resubmitting analytical samples. Secondly, several databases were used individually to model the experiments. Finally, a modification to the standard flowsheet was applied. The original solids were separated into layers and the brine fractions were set to generate the nitrate concentrations of the effluent collected. The number of layers generated from the solids

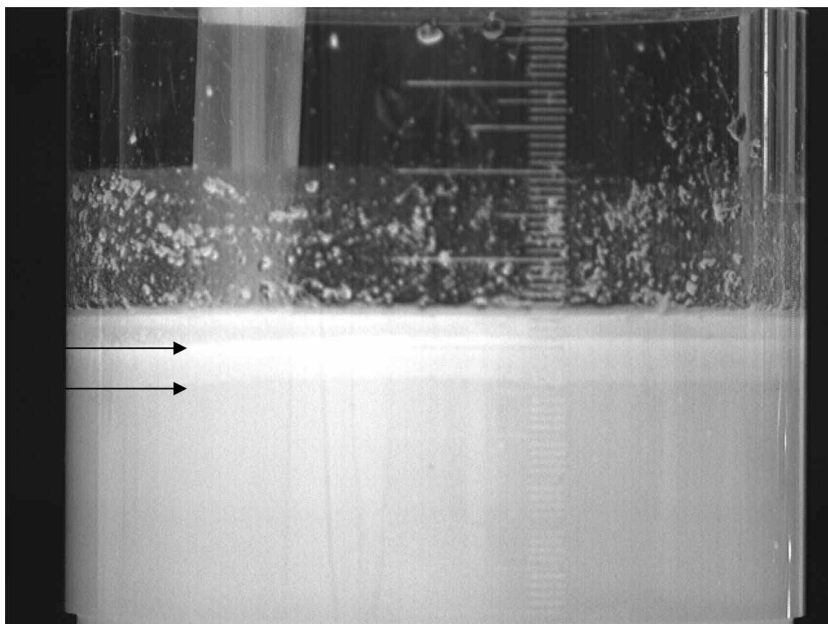


Figure 9. SRS Tank 37H simulant layer shown during dilution portion of experiment.

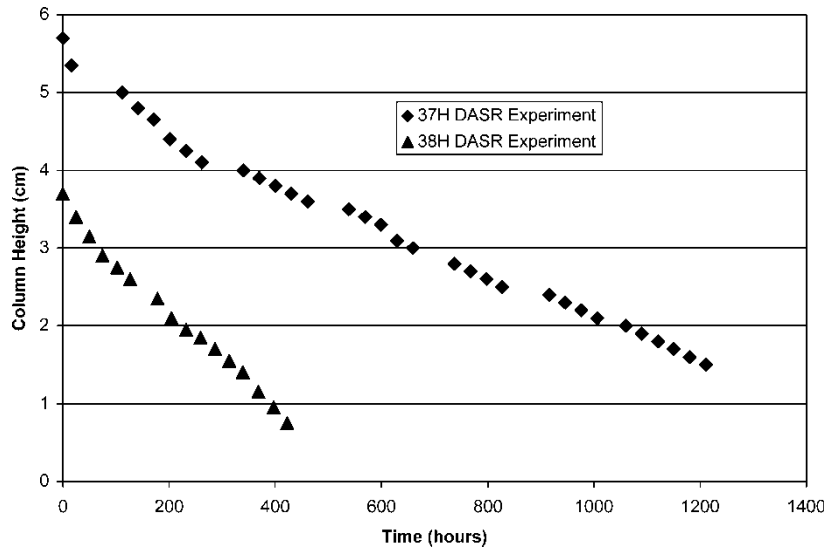


Figure 10. Column height against experiment time for 37H and 38H simulant comparison.

was dependent upon the nitrate fraction concentrations obtained during the experiment.

By separating the solids into layers based upon the nitrate ion concentrations and using the modified flowsheet approach, profiles for both nitrate and carbonate ion dissolution demonstrated an improved correlation

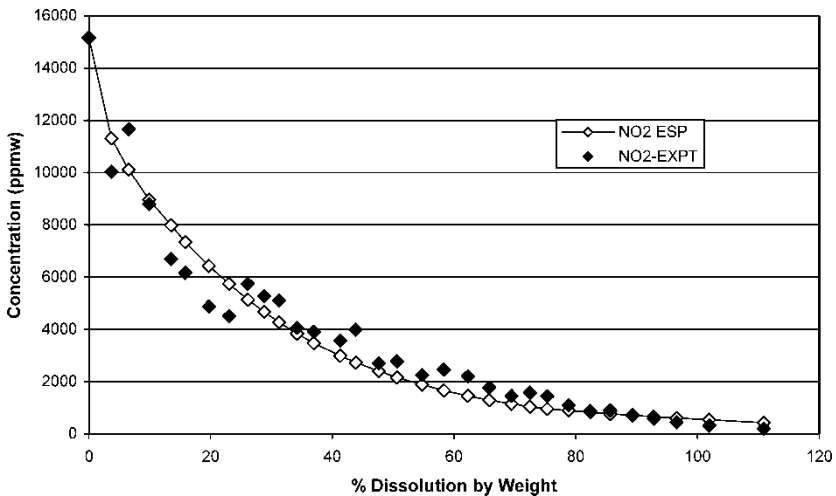


Figure 11. Comparison of experimental and predicted NO_2 ion concentrations (ppmw) for Tank 37H experiment-standard flowsheet.

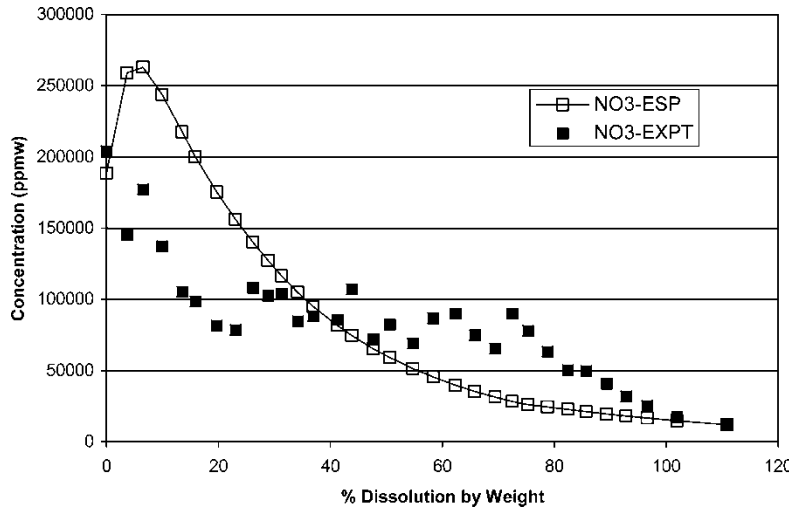


Figure 12. Comparison of experimental and predicted NO_3^- ion concentrations (ppmw) for Tank 37H experiment-standard flowsheet.

between experimental results and the model predictions. These profile comparisons are shown in Figs. 14 and 15.

The primary observation regarding the behavior of the 37H salt cake simulant relates to the formation of an impervious layer within the column.

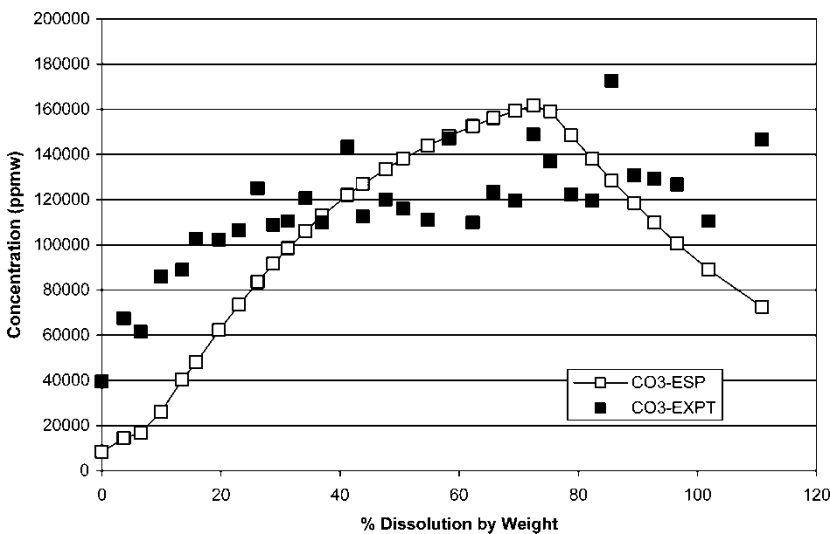


Figure 13. Comparison of experimental and predicted CO_3^- ion concentrations (ppmw) for Tank 37H experiment-standard flowsheet.

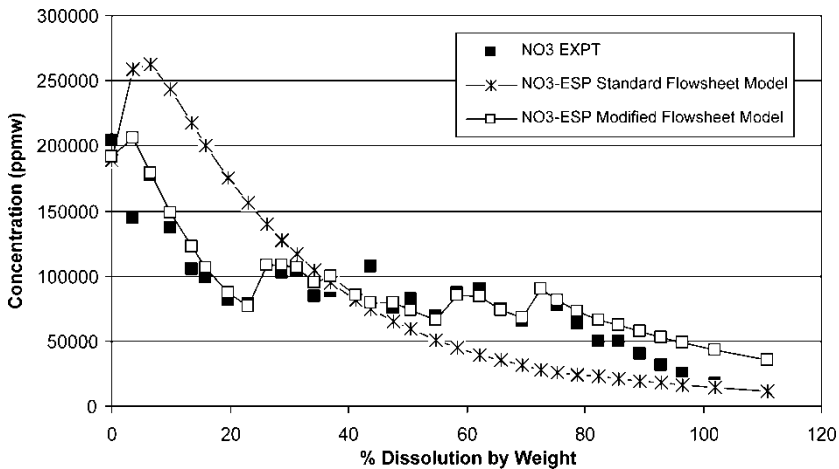


Figure 14. Comparison of experimental and predicted NO_3^- ion concentrations (ppmw) for Tank 37H experiment-standard and modified flowsheets.

A similar event was encountered previously with respect to the formation of an $\text{Al}(\text{OH})_3$ layer with a Hanford composition (9). In practice it would take a considerable mass of cancrinite or gibbsite to stretch over the diameter to a waste tank; however, the layer formation can clearly result in schedule slippage and in the need to employ more aggressive means prior to formally closing the tanks.

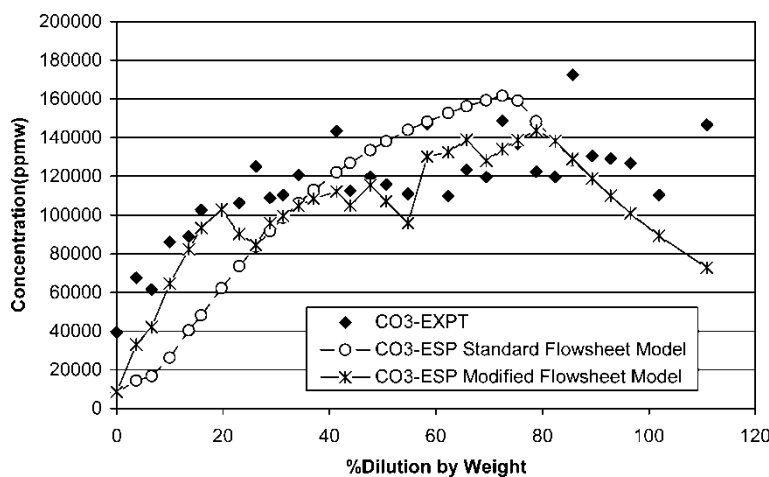


Figure 15. Comparison of experimental and predicted CO_3^- ion concentrations (ppmw) for Tank 37H experiment-standard and modified flowsheets.

CONCLUSIONS

The DASR experimental results for 38H and 37H indicate that flowsheet refinement may be necessary when considering salt cake dissolution operations where the bulk of the interstitial liquor has been drained from the waste. Large variations for nitrite and other aqueous ions such as aluminum, sulfate, and phosphate concentrations may be expected; however, for the predominant solids such as sodium nitrate and sodium carbonate monohydrate, the resulting concentration profiles will be little changed. The effect will influence all of the anions that primarily partition to the aqueous phase. In the case of cesium, increased activities over those expected and based entirely on dilution of the aqueous phase may well result thereby resulting in the need for additional separations.

Another insight relates to the ultimate need to consider tank waste hydrology in accurately modeling the dissolution and retrieval processes. Typical dissolution/dilution response curves were not observed for the tank 38H simulant. Here the concentration of nitrate decreased and then increased as if additional solids were undergoing dissolution. Changes in the concentration profiles can be accounted for by developing the proper flowsheet; however, in this work, the change in the flowsheet was accomplished after the fact. Knowledge of the distribution of the interstitial liquor within the tank, presumably from non-contact activity measurements for Cs¹³⁷, would be useful in this respect along with results of hydraulic modeling studies. Alternately, a series of flowsheets beginning with the simple configuration and progressing to include additional layers can be developed. In this way, potential ranges for specific ion concentrations, which affect downstream activities and waste acceptance criteria (corrosion and saltstone), can be established.

REFERENCES

1. SRS Environmental management program performance management plan. (2002) WSRC-RP-2002-00245, Rev 6, August 7.
2. Brooke, J.N., Stahlie, K., and Peters, J.F. (1999) Hydrological methods can separate cesium from nuclear waste salt cake. WSRC-TR-99-00358, July.
3. SRS planned disposition of material in the savannah river site high level waste system. (2003) WSRC-RP-2003-00323, March 17.
4. Lindner, J.S., Antonyraj, A., Durve, T., and Toghiani, R.K. (2002) Solids formation. In DIAL Technical Progress Report 40395R14. Diagnostic Instrumentation and Analysis Laboratory, Mississippi State University, Mississippi State, MS.
5. Martino, C.J., Poirier, M.R., and Gregory, N.E. (2002) Salt cake dissolution simulant tests. WSRC-TR-2002-00387, Rev 0, December 11.
6. Martino, C.J., Nichols, R.L., McCabe, D.J., and Hansen, E.K. (2004) Tank 38H salt cake core and supernate sample analysis. WSRC-TR-2004-00129, Rev. 0, April 8.

7. Pike, Jeff. Personal communication.
8. Togiani, R.K., Smith, L.T., Phillips, V.A., Jung, M.H., Selvaraj, D., and Lindner, J.S. (2005) Improved process chemistry for legacy nuclear waste remediation: development of the DBLSLTDB. *14th Symposium on Separation and Science Technology for Energy Applications*.
9. Antonyraj, A., Durve, T., Togiani, R.K., Lindner, J.L., and Hunt, R. (2003) Salt cake dissolution studies in support of single-shell tank retrieval. *Waste Management '03*: Tucson, AZ.
10. Jantzen, C.M., Swingle, R.F., and Smith, F.G. (2003) Impact of zeolite transferred from Tank 19F to Tank 18F on DWPF vitrification of sludge batch 3 (U). WSRC-TR-2002-00288, Rev. 0, September 18.
11. Addai-Mensah, J., Li, J., Zbik, M., and Rosencrance, S. (2002) The chemistry, crystallization, physiochemical properties and behavior of sodium aluminosilicate solid phases: Final Report, WSRC-MS-2002-00907, November 20.